Conformation and Dynamics of an F_{ab}'-Bound Peptide by Isotope-Edited NMR Spectroscopy†

P. Tsang,*,‡ M. Rance, T. M. Fieser,§ J. M. Ostresh,∥ R. A. Houghten,⊥ R. A. Lerner, and P. E. Wright*
Department of Molecular Biology, MB-2, The Scripps Research Institute, La Jolla, California 92037
Received November 5, 1991

ABSTRACT: The dynamics and conformation of the peptide antigen MHKDFLEKIGGL bound to the F_{ab}' fragment of the monoclonal antipeptide antibody B13A2, raised against a peptide from myohemerythrin, have been investigated by isotope-edited NMR techniques. The peptides were labeled with ^{15}N (98%) or ^{13}C (99%) at the backbone of individual amino acid residues. Well-resolved amide proton and nitrogen backbone resonances were obtained and assigned for eight of the 12 residues of this bound peptide. Significant resonance line width and chemical shift differences were observed. The ^{15}N and ^{1}H line width variations are attributed to differential backbone mobilities among the bound peptide residues which are consistent with the previously mapped epitope of this peptide antigen. Local structural information was obtained from isotope-directed NOE studies. The approximate distances associated with the experimental NOEs were estimated on the basis of a theoretical NOE analysis involving the relative integrated intensities of the NOE and source peaks. In this way, the sequential NH–NH NOEs obtained for seven of the F_{ab}'-bound peptide residues were shown to correspond to interproton separations of ~3 Å or less. Such short distances indicate that the backbone dihedral angles of these residues are in the α rather than the β region of ϕ,ψ conformational space; the peptide most likely adopts a helical conformation from F_5 to G_{11} within the antibody combining site. The significance of these results with respect to the type and extent of conformational information obtainable from studies of high molecular weight systems is discussed.

A fundamental challenge in the field of immunochemistry is to obtain a detailed understanding of the molecular basis for antibody–antigen recognition. The interaction of antibodies with peptide antigens is of particular interest due to the development of antipeptide antibodies as important tools in medicine and biology (Lerner, 1982, 1984; Walter, 1986; Arnon, 1986; Steward & Howard, 1987). Among the antipeptide antibodies raised against specific peptide immunogens, a number have been observed to bind both the peptide and the protein from which the peptide sequence was derived. The structural basis for cross-reactivity with the cognate sequence in the protein antigen (Lerner, 1984; Van Regenmortel, 1987) is not well understood, although X-ray crystallographic studies of antipeptide antibodies and their complexes with peptide antigens are beginning to provide valuable insights (Stanfield et al., 1990; Wilson et al., 1991).

Nuclear magnetic resonance (NMR) spectroscopy offers unique opportunities for studying the structure and dynamics of antibody–antigen complexes. The largest antibody fragment amenable to detailed NMR analysis is the F_{ab}[1] or F_{ab}' fragment which is easily obtained by proteolytic cleavage. The high molecular mass of the F_{ab} (~50 kDa) means that most NMR studies to date have focussed on the conformation of the bound antigen (Anglister et al., 1989; Zilber et al., 1990; Glasel & Borer, 1986; Glaudemans et al., 1990) although, with the aid of selective antibody deuteration, information on the structure of the combining site can be obtained (Anglister et al., 1987; Anglister, 1990a; Zilber et al., 1990).

NMR studies of peptide complexes of the F_{ab} fragments of several antipeptide antibodies have been reported recently (Anglister et al., 1988, 1990b; Levy et al., 1989; Ito et al., 1987; Tsang et al., 1988, 1990a). Detailed investigations, using transferred NOE techniques, of complexes of cholera toxin peptides with antipeptide F_{ab}s have been reported by Anglister and co-workers (Anglister et al., 1988, 1989; Zilber et al., 1990). These methods rely upon the indirect characterization of antigen–antibody interactions via the NMR spectrum of the free antigen. A prerequisite of these methods is that relatively fast exchange of the antigen between the free and bound states must occur, and it is therefore applicable, in general, only to antibody–antigen complexes of relatively low affinity. In addition, extreme caution is necessary in transferred NOE experiments to avoid confusion between specific and nonspecific binding effects. Obviously, methods which allow direct observation of the resonances of the bound peptide antigen would be of considerable value.

NMR studies of high molecular mass systems, such as F_{ab}'-peptide complexes of molecular mass ~55 kDa, have been greatly facilitated by the development of isotope-edited NMR techniques (Griffey & Redfield, 1987; Wagner, 1989; Otting & Wüthrich, 1990; Fesik et al., 1988; Tsang et al., 1991). Using these methods, it is possible to directly observe specific resonances of a bound antigen when the exchange (off) rate of the antigen is slow with respect to the chemical shift time scale. In the present study, isotope-edited NMR spectroscopy

† This work was supported by NIH Grant CA 27498 and NSF Grant DMB-8903777.
* Authors to whom correspondence should be addressed.
‡ Current address: Department of Chemistry, University of Cincinnati, Cincinnati, OH 45221.
§ Amylin Corporation, 9373 Towne Centre Drive, San Diego, CA 92121.
∥ Multiple Peptide Systems, 3550 General Atomics Court, San Diego, CA 92121.
⊥ Torrey Pines Research Institute for Molecular Studies, 3550 General Atomics Court, San Diego, CA 92121.

[1] Abbreviations: 1D, one dimensional; 2D, two dimensional; COSY, correlated spectroscopy; NOE, nuclear Overhauser enhancement; NOESY, nuclear Overhauser enhancement spectroscopy; FID, free induction decay; SED, spin echo difference; IgG, immunoglobulin G; F_{ab}', pepsin-derived antibody antigen-binding fragment consisting of light and heavy chain variable domains, the light chain constant domain, and the first constant domain of the heavy chain; F_v, antibody variable light (V_L) and heavy (V_H) chain regions of antigen-binding fragment (F_{ab}).

0006-2960/92/0431-3862$03.00/0

is employed to characterize directly the bound state of a 12-residue peptide antigen in its complex with an antipeptide F_{ab}'. Through selective incorporation of stable isotopes such as ^{15}N and ^{13}C into the peptide and the use of isotope-editing techniques, the bound peptide antigen (whose exchange rate is slow with respect to the chemical shift time scale) is selectively examined.

The particular monoclonal antipeptide antibody employed, B13A2 (henceforth called A2 for brevity), was raised against a 19-residue peptide immunogen coupled to keyhole limpet hemocyanin (Fieser et al., 1987). The sequence of this peptide corresponds to residues 69–87 of *Themiste zostericola* myohemerythrin (Sheriff et al., 1987). The A2 antibody binds to the 19-residue peptide and also cross-reacts with the protein myohemerythrin (Fieser et al., 1987). The 12-residue antigen used in the present NMR study corresponds to a truncated version (residues 76–87) of the original peptide. The relative affinities of A2 for both peptides are similar (T. M. Fieser, unpublished results) and are both higher than the binding constant of 2×10^7 M^{-1} for myohemerythrin (Fieser et al., 1987). The conformational and dynamic information regarding this complexed peptide antigen obtained through the application of isotope-edited NMR techniques is expected to contribute to the understanding of the protein/peptide antigen recognition process by antipeptide antibodies in general.

Materials and Methods

The mouse monoclonal antibody A2 (IgG1) was raised against a synthetic peptide corresponding to residues 69–87 of *T. zostericola* myohemerythrin coupled to a carrier protein, keyhole limpet hemocyanin (KLH). The antibody was purified and enzymatically cleaved with pepsin to produce F_{ab}' as described earlier (Fieser et al., 1987; Tsang et al., 1988). Typical NMR samples contained F_{ab}' at concentrations between 0.2 and 1.0 mM in a 0.1 M sodium deuteroacetate buffer, pH 5, in 90% H_2O/10% D_2O (Tsang et al., 1988).

Peptide antigens of sequence $M_1H_2K_3D_4F_5L_6E_7K_8I_9$-$G_{10}G_{11}L_{12}$-$NH_2$ were synthesized using solid-phase methods (Houghten, 1985) and purified to greater than 95% purity by HPLC. The peptides were synthesized using ^{13}C- or ^{15}N-labeled amino acids for incorporation at specific sites. A series of peptides was produced with single or double labels at the amide nitrogen of D_4, F_5, L_6, E_7, K_8, I_9, G_{10}, and G_{11}. One peptide containing $^{13}C_\alpha$-labeled glycine at residue G_{10} was also synthesized. The labeled amino acids (>98% isotopic enrichment) were obtained from Merck Sharpe & Dohme and Cambridge Isotope Laboratories. The free amino acids were converted into the corresponding *t*-Boc derivatives using standard procedures (Itoh et al., 1975; Benoiton, 1962; Erickson & Merrifield, 1973). The peptide molecular weight was checked by mass spectrometry and its sequence by homonuclear COSY (Aue et al., 1976) and NOESY (Jeener et al., 1979) experiments.

The labeled peptides were titrated into the F_{ab}' samples as described previously (Tsang et al., 1988). Stock solutions (3–6 mM) of peptide in the same buffer as that of the F_{ab}' were used, and the titrations were monitored by 1D reverse-detection NMR techniques. The ^1H chemical shifts were referenced to internal dioxane and ^{15}N-labeled formamide was used as an external reference for ^{15}N chemical shifts. The ^{13}C chemical shift scale was referenced to hypothetical internal TSP (Live et al., 1984; Bax & Subramanian, 1986).

The pulse sequences employed to acquire one- and two-dimensional spectra of these complexes correspond to versions of the spin echo difference (SED) experiment (Griffey & Redfield, 1987; Tsang et al., 1991), the heteronuclear multiple-quantum coherence (HMQC) pulse sequence of Bax et al. (1983), and the heteronuclear single-quantum coherence (HSQC) sequence of Bodenhausen and Ruben (1980). These sequences were modified to suppress the residual water resonance intensity. This was accomplished via the use of a 90°_x–τ–90°_x sequence (Plateau & Guéron, 1982) as the initial proton pulse or through solvent presaturation. Spectra were acquired using 5-mm reverse-detection probes on Bruker AM spectrometers at 500 and 600 MHz ^1H frequencies and ^{15}N frequencies of 50.7 and 60.8 MHz. NMR spectra from ^{13}C-labeled peptides and peptide–F_{ab}' complexes were recorded at 150.9 MHz. ^{13}C and ^{15}N decoupling was accomplished using a WALTZ-16 sequence (Shaka et al., 1983) during acquisition. The Bruker low-power "ROESY" output was used as input to an ENI-525LA broad-band amplifier for X-nucleus decoupling. Unless otherwise stated, all spectra were recorded at 308 K.

Two-dimensional HSQC data sets were obtained from F_{ab}'–peptide complexes containing peptides labeled with ^{15}N at residues D_4, F_5, E_7, G_{10}, and G_{11}. The interferograms of the HSQC data were fitted using a nonlinear least-squares algorithm to estimate the T_2^* values for the ^{15}N resonances.

One- and two-dimensional isotope-directed NOE spectra were acquired using the pulse sequence of Rance et al. (1987), modified to incorporate either a jump–return pulse (Plateau & Guéron, 1982) as the final observe pulse, solvent presaturation with a homo-spoil pulse, or a spin-lock purge pulse (Messerle et al., 1989) to suppress the water resonance. The observable magnetization in this experiment originates from the "source" proton which is bound to an X nucleus (^{15}N or ^{13}C) and is transferred during the mixing time to nearby protons via dipolar cross-relaxation processes. The source resonance occurs in ω_1 at the ^{15}N chemical shift of the labeled nitrogen and at the ^1H chemical shift of the attached proton in ω_2. Due to the X–H heteronuclear scalar coupling, source peaks appear as singlets if X-nucleus decoupling is employed during acquisition or as doublets otherwise. NOEs occurring between the source proton and nearby protons give rise to singlet peaks which appear at the X-nucleus frequency of the labeled residue in ω_1 and at the ^1H frequency of the nearby proton in ω_2. All NOE spectra obtained from the F_{ab}'–peptide complexes were recorded at 600 MHz at 308 K using mixing times of 30–50 ms.

Calculations of NOE buildup curves were carried out using the Fortran simulation program NOECAL (M. Rance, unpublished). This program implements a full relaxation matrix analysis for a system of dipolar-coupled spin $^1/_2$ nuclei (Bodenhausen & Ernst, 1982; Keepers & James, 1984; Olejniczak et al., 1986). Methyl group rotation is treated by a general model in which the methyl protons make random jumps among three sites (Tropp, 1980; Olejniczak, 1989). The program allows simulation of the cross-relaxation behavior of a specified nucleus with the remaining nuclei in the system of interest; also included is the capability to set specific cross-relaxation rates to zero in order to distinguish between direct and indirect contributions to magnetization transfer. The proton geometries employed for the NOE simulations were obtained by introducing protons with standard geometries and bond lengths into the crystallographic coordinate files of the proteins *T. zostericola* myohemerythrin (Sheriff et al., 1987) and poplar plastocyanin (Guss & Freeman, 1983). This was achieved through use of the vectorized version of the program AMBER (Version 3.3) (Singh et al., 1986).

Results and Discussion

Peptide Interactions with F_{ab}'. One-dimensional reverse-

Table I: ^{15}N-Labeled Amide Residues of the C-Helix Peptide: MHKDFLEKIGGL-NH_2

	^{1}H chemical shift (±0.03 ppm)		^{15}N chemical shift (±1 ppm)		line width (bound)		
residue	free	bound	free	bound	^{1}H[a]	^{15}N[b]	^{15}N T_2* (±1 ms) bound
D_4	8.38	9.66	124	131	31	15	21
F_5	8.10	8.93	123	128	47	18	18
L_6	8.12	8.56	126	118	42		
E_7	8.16	7.05	124	120	38	13	25
K_8	8.19	7.70	125	123	35		
I_9	8.07	7.05	124	113	38		
G_{10}	8.44	7.50	116	113	25	10	31
G_{11}	8.20	7.72	111	110	18	5	58

[a] ±2 Hz. [b] Calculated from ^{15}N T_2*.

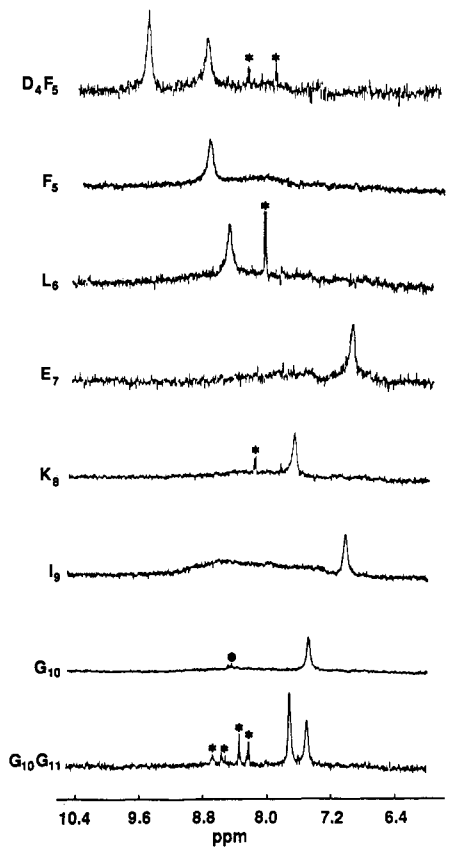

FIGURE 1: ^{15}N-edited ^{1}H spectra recorded (with SED sequence, 1–1 initial proton pulse and no ^{15}N decoupling) for a series of ^{15}N-labeled peptide–F_{ab}′ complexes. All spectra were recorded at 308 K and 500 MHz (^{1}H frequency) and 50.66 MHz (^{15}N frequency). Peptides were singly or doubly ^{15}N-labeled at the residues indicated to the left of each spectrum. The D_4 resonance was assigned from peptide doubly labeled at this and residue F_5 (top spectrum). The G_{11} resonance was assigned on the basis of the spectrum (bottom) of F_{ab}′ complexed with G_{10}, G_{11} ^{15}N-labeled peptide. A total of 12 000–75 000 transients were collected per FID using typical acquisition times of 0.33–0.44 s and a recycle delay of ~1 s. The FIDs were transformed without prior apodization. Additional, smaller resonances due to free peptide are indicated by asterisks.

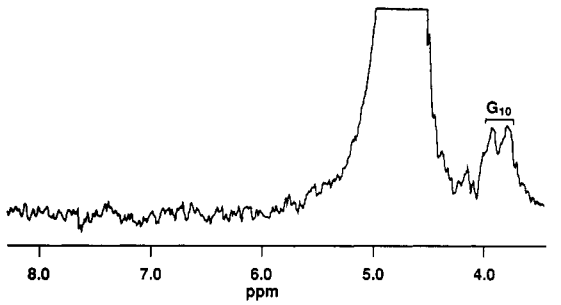

FIGURE 2: SED ^{13}C-edited spectrum (acquired with ^{13}C-decoupling and solvent presaturation) recorded from sample of F_{ab}′ complexed with $^{13}C_\alpha$-labeled G_{10} peptide. Data were obtained at 308 K and 600 MHz (^{1}H) and 150.9 MHz (^{13}C) Larmor frequencies. A total of 1024 transients were acquired for this FID using a recycle delay of 2.2 s and a 0.4-s acquisition time. Lorentzian broadening (10 Hz) was applied to the FID prior to Fourier transformation. Approximate concentrations of F_{ab}′ and peptide were 0.6 mM (F_{ab}′) and 0.3 mM (peptide).

detected SED spectra recorded from complexes of the A2 F_{ab}′ with ^{15}N-labeled myohemerythrin peptides are shown in Figure 1. The titration of each F_{ab}′ sample with a specifically labeled peptide was monitored by reverse-detection NMR techniques. In all cases, resonances corresponding to the bound peptide were observed first upon addition of peptide to the F_{ab}′ samples. In the presence of excess peptide, resonances were also observed due to the free form of the peptide, thus indicating that the peptide chemical exchange rate (i.e., k_{off}) is slow with respect to the chemical shift time scale (Tsang et al., 1988). The resonances shown in Figure 1 are (except where noted) due to the F_{ab}′-bound peptide. The chemical shifts of most of the ^{1}H and ^{15}N backbone resonances are unique. Two-dimensional ^{1}H–^{15}N HMQC experiments provided the ^{15}N chemical shifts of the amide nitrogens. The ^{1}H and ^{15}N chemical shifts of the various bound and free peptide resonances are summarized in Table I. The chemical shift differences between bound and free peptide range from 0.4 to 1.3 ppm for ^{1}H and from 1 to 7 ppm for ^{15}N (see Table I). From the free vs bound ^{15}N resonance frequency differences, the rate of peptide dissociation from the F_{ab}′ is estimated to be slower than ~15 s^{-1}.

The α-proton resonances of residue G_{10} were assigned from a 1D ^{13}C-edited spectrum (Figure 2) of the complex of F_{ab}′ with peptide labeled with 99% ^{13}C at the C_α position of G_{10}. In an NMR titration of this sample, two resonances at 3.98 and 3.83 ppm appeared when peptide was added to the F_{ab}′ sample, and their intensities increased with further added peptide. The ^{13}C resonance was at 46.4 ppm (relative to TSP). The chemical shifts of these resonances are characteristic of glycine.

For most residues of the peptide, significant chemical shift changes occur upon binding to the F_{ab}′. Unfortunately, interpretation of these chemical shift changes in terms of specific conformational rearrangements upon peptide binding is not possible at this time. Quantitative interpretation of the chemical shift for a given nucleus requires evaluation of the contributions from aromatic ring current shifts, hydrogen-bonding effects, electrostatics, and other factors (Wüthrich, 1986) which influence the nuclear environment in the bound state. Clearly, this is not possible without independent knowledge of the three-dimensional structure of the antibody–peptide complex. In qualitative terms, however, the chemical shift differences observed between the free and bound

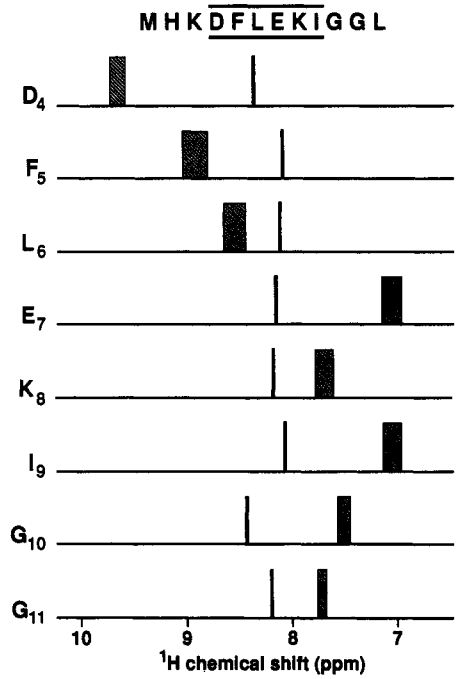

FIGURE 3: Schematic representation of the frequencies and line widths of the free and bound peptide ^1H resonances of the complexes whose experimental spectra are shown in Figure 1. The residue associated with each graph is indicated to the left. The solid and striped bars represent the free and bound peptide resonances, respectively. The horizontal position of each bar corresponds to the resonance frequency, while the breadth of each bar reflects resonance line width (each solid bar corresponds to 5 Hz, not to scale with the chemical shift axis). The peptide sequence is shown at the top of this figure; underlined residues correspond to the epitope of this peptide antigen.

forms of the peptide indicate that it binds strongly and specifically to the F_{ab}' and undergoes significant conformational changes as a result. The temperature coefficients measured (over the temperature range of 278–313 K) for the amide proton resonances of several residues of the bound peptide were significantly reduced to ~−4 ppb/K from the value of ~−6 ppb/K found for the corresponding residues of the free peptide (H. J. Dyson and P. E. Wright, unpublished observations). The reduced temperature coefficients for the bound peptide clearly reflect increased solvent protection of the peptide and/or hydrogen-bond formation upon binding to the F_{ab}'. This hydrogen bonding could be either intramolecular (within the peptide) or intermolecular (within the peptide–F_{ab} complex). The behavior of both the temperature coefficients and the chemical shifts indicates that significant conformational differences exist between the free and bound states of the peptide.

Dynamics of the F_{ab}'-Bound Peptide. The amide proton resonance line widths were measured from the 1D ^{15}N-edited spectra of the labeled peptide–F_{ab}' complexes and are included in Table I. Figure 3 shows in schematic form the chemical shift and line width changes between the free and bound forms of the peptide. Significant variations of the resonance line widths (which range from 18–47 Hz) are observed among the amide proton resonances of the F_{ab}'-bound peptide. The resonance line widths increase in the following order: G_{11} (18 Hz), G_{10} (25 Hz), D_4 (31 Hz), K_8 (35 Hz), I_9, E_7 (38 Hz), L_6 (42 Hz), and F_5 (47 Hz). Since the NH–C$^\alpha$H scalar couplings are unknown for the bound peptide, it was not possible to distinguish this contribution to the observed line width from those due to homogeneous and inhomogeneous line broadening; however, the homonuclear scalar couplings are expected to be in the range of 3–10 Hz. The amide proton resonance line widths for the free peptide were measured to be 5 Hz or less.

Amide ^{15}N T_2^* values were estimated for the D_4, F_5, E_7, G_{10}, and G_{11} residues of the F_{ab}'-bound peptide. This was accomplished through nonlinear least-squares fitting of the interferograms from 2D HSQC data sets recorded from the ^{15}N-labeled peptide–F_{ab}' complexes; no proton decoupling was employed during the ^{15}N evolution period. The T_2^* values are 21 (D_4), 18 (F_5), 25 (E_7), 31 (G_{10}), and 58 ms (G_{11}), and the associated ^{15}N resonance line widths are G_{11} (5 Hz), G_{10} (10 Hz), E_7 (13 Hz), D_4 (15 Hz), and F_5 (18 Hz) (see Table I). The analogous line widths for the free peptide were less than 2 Hz.

The variations in the observed ^1H and ^{15}N line widths provide valuable insights into the dynamics of the F_{ab}'-bound peptide. The simplest explanation for these data is variation in backbone mobility at different residues of the bound peptide. The amide proton resonance line width for a peptide residue immobilized in the peptide–F_{ab}' complex would be expected to be in the range of 40–50 Hz (Tsang et al., 1988). In the same situation, the backbone ^{15}N resonance line width measured in a HSQC experiment, with no proton decoupling during the ^{15}N evolution period, is estimated to be ~15 Hz; this estimate was determined by calculating the dipolar and chemical shift anisotropy contributions to the transverse relaxation of a ^{15}N–^1H spin pair and includes a term to account for coupling to additional protons (Goldman, 1984; Palmer et al, 1991, 1992). Thus, a comparison of the line widths expected for a residue immobilized on the F_{ab} with the experimentally determined values for the peptide strongly supports a model in which the residues in the vicinity of F_5 are relatively immobilized in the F_{ab} binding site. In addition, there appears to be some mobility at the carboxyl terminus of the peptide which gives rise to the observed line narrowing for the glycine resonances. The fact that similar trends are observed for both ^1H and ^{15}N line widths gives confidence that differential backbone mobility among the residues of the bound peptide is indeed responsible for the variations in line width, although a detailed and complete relaxation analysis, including T_1, T_2, and heteronuclear NOE measurements, would be necessary to fully characterize the dynamics of the bound peptide.

For both ^1H and ^{15}N, the broadest resonances originate from amino acids within the epitope, residues DFLEKI (Fieser et al., 1987; Scott & Smith, 1990). The amino acids comprising the epitope are essential for high-affinity binding to the F_{ab}', which implies that they participate in strong and specific interactions with the backbone or side chains forming the combining site of the antibody. A likely consequence of this is a significant decrease in the conformational freedom of the bound peptide in the epitope region. The observed pattern of line widths is readily explained by a model in which the residues within the epitope are immobilized relative to those that lie outside the antibody combining site. In such a model, considerable line broadening would be expected for the resonances of D_4, F_5, L_6, E_7, K_8, and I_9, i.e., all of the residues that constitute the immunologically defined epitope. In contrast, the resonances of G_{10} and G_{11}, which lie outside the epitope, are much less broadened, suggesting that these residues retain some degree of conformational flexibility when bound to the antibody. Hence, isotope-edited NMR allows specific identification of those bound peptide residues whose mobilities are most affected by antibody binding, i.e., which lie within the epitope. This NMR epitope determination is possible only due to the ability to *directly* detect the bound peptide resonances.

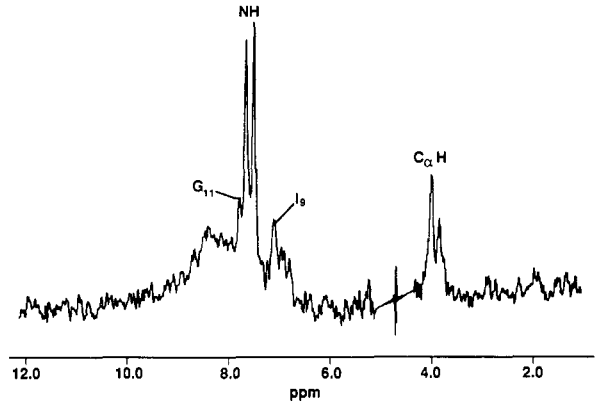

FIGURE 4: ^{15}N-edited NOE spectrum obtained with a 50-ms mixing time for a complex containing peptide labeled with ^{15}N at residue G_{10}. The doublet (at 7.44 and 7.58 ppm) corresponds to the amide proton of G_{10} (no ^{15}N decoupling). The two resonances at 7.05 and 7.72 ppm in this spectrum have been assigned (as described in text) to the amide protons of I_9 (7.05 ppm) and G_{11} (7.72 ppm). The spectrum was recorded with a 0.4-s acquisition time at 308 K and 600 MHz (^1H) and 60.8 MHz (^{15}N) Larmor frequencies. A total of ~39 000 transients were collected. Water resonance suppression accomplished via a spin-lock purge pulse in addition to a postacquisition Hilbert transformation procedure (Tsang et al., 1990c). The low-intensity hump (from ~9–6.5 ppm) is due to the F_{ab}' natural abundance ^{15}NH intensity. The F_{ab}' and peptide concentration in this sample was ~1 mM. A 15-Hz Lorentzian broadening was applied to the FID prior to Fourier transformation.

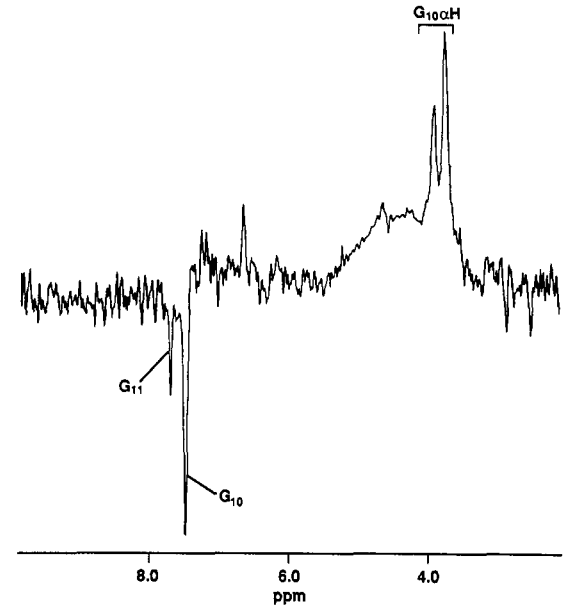

FIGURE 5: Row from a 2D ^{13}C-directed, 50-ms mixing time NOE experiment obtained (with ^{13}C decoupling) from a sample of F_{ab}' complexed with $^{13}C_\alpha$-labeled G_{10} peptide. Data were processed using a low-pass digital filter (Marion et al., 1989) which gives rise to the low-level hump around 4–5 ppm. Resonances at 3.98 and 3.83 ppm are due to the G_{10} α-protons. NOE resonances are observed at 7.72 and 7.50 ppm; due to the jump–return sequence employed as the final read pulse, these peaks are inverted relative to the G_{10} α-proton "source" peaks. Data were acquired using ^{13}C and ^1H frequencies of 150.9 and 600 MHz, respectively, at 308 K. The acquisition time and recycle delay used to collect data were 0.4 and 2.4 s, respectively. A total of 52 t_1 × 16 384 t_2 points were collected for this 2D data matrix with 1024 acquisitions per t_1 point. Dimensions of processed 2D data matrix were 128 × 4096. The F_{ab}' and peptide concentrations were about 0.6 and 0.3 mM, respectively.

Crystallographic studies of a related F_{ab}'–peptide complex (Stanfield et al., 1990) lend support to our interpretation of the line width data. The amino acids within the epitope of the peptide antigen were found in well-defined secondary structure within the antibody combining site, while no electron density was observed for residues outside the epitope. This could result either from static disorder or from greatly increased mobility of the residues outside the epitope. Although it is not possible to determine from the crystallographic data alone whether this disorder is static or dynamic in nature, NMR techniques do permit such a distinction.

Conformational Studies of the F_{ab}'-Bound Peptide. To obtain information on the conformation of the bound peptide, 1D and 2D isotope-directed NOE experiments were conducted upon the various labeled peptide–F_{ab}' complexes. An example of a ^{15}N-coupled, isotope-directed NOE spectrum (50-ms mixing time) obtained from F_{ab}' complexed with ^{15}N-labeled G_{10} peptide is shown in Figure 4. The source peak due to the amide proton of the labeled G_{10} residue is the large doublet at 7.41 and 7.60 ppm. Two resonances which occur at 7.72 and 7.05 ppm result from NOEs between the G_{10} amide proton and nearby amide or aromatic protons. The two resonances at 3.83 and 3.98 ppm result from NOEs between the G_{10} amide proton and aliphatic protons. A similar pattern of NOEs was obtained from a 2D ^{13}C-edited NOE spectrum (50-ms mixing time) of a complex containing $^{13}C_\alpha$-labeled G_{10} peptide. Figure 5 shows a row from this spectrum with the G_{10} α-protons at 3.98 and 3.83 ppm and the two NOE resonances at 7.72 and 7.50 ppm.

Two-dimensional ^{15}N-edited NOE spectra of the complexes of the F_{ab}' with peptides labeled with ^{15}N at the amides of L_6 through G_{11} are shown in Figure 6. The NOE data obtained from the complex containing ^{15}N-labeled L_6 peptide are shown in Figure 6A. The L_6 amide proton doublet is centered at 8.56 ppm. Further peaks at ^1H frequencies of 7.05 and 8.93 ppm and the common ω_1 frequency of 118 ppm (L_6 ^{15}N chemical shift) are apparent; these reflect NOEs between the L_6 amide proton and nearby amide/aromatic protons. Figure 6B shows part of the ^{15}N-edited NOE spectrum of the E_7-labeled peptide-F_{ab}' complex. The E_7 amide proton doublet is centered at 7.05 ppm; the corresponding ^{15}N frequency is 120 ppm. Two NOE cross peaks are seen at 7.70 and 8.56 ppm in ω_2. The amide proton doublet of K_8 occurs at 123 ppm (^{15}N) and is centered at 7.70 ppm (^1H), with an NOE cross peak at ~7.05 ppm (Figure 6C). The amide proton doublet resonance of residue I_9 is centered at 7.05 ppm (^1H) and 113 ppm (^{15}N) (Figure 6D). NOEs occur at this ^{15}N frequency and at ^1H frequencies of 7.50 and 7.70 ppm. The NOE spectrum recorded for a F_{ab}' complex with peptide labeled at G_{10} is shown in Figure 6E and contains a doublet centered at 7.50 ppm which represents the amide proton resonance of this residue. Figure 6F shows the spectrum recorded from a complex containing peptide labeled at both G_{10} and G_{11}; the G_{11} amide proton doublet is centered at 7.72 ppm. The corresponding ω_1 (^{15}N) frequencies for the glycine residues are 113 (G_{10}) and 110 ppm (G_{11}). The NOE peak in common to the spectra of Figure 6E,F occurs at 7.05 ppm (^1H) and 113 ppm (^{15}N). In Figure 6E, an additional NOE peak is observed at 7.72 ppm. In Figure 6F, two unique resonances are seen at 7.41 and 7.81 ppm in ω_2; these ^1H frequencies coincide with the upfield and downfield components of the G_{10} and G_{11} NH doublet resonances, respectively. For all residues examined, the one-bond ^1H–^{15}N scalar coupling was measured to be ~90 Hz.

In the spectra shown in Figure 6, two NOE cross peaks are observed in the amide/aromatic proton region for all of the peptide–F_{ab}' complexes, except that labeled with ^{15}N at K_8 for which only a single NOE is found at ~7.05 ppm in ω_2. In all cases, the observed NOE cross peaks are at proton chemical shifts that correspond to adjacent amide protons of the peptide (Table I), i.e., represent sequential NH–NH NOEs. The

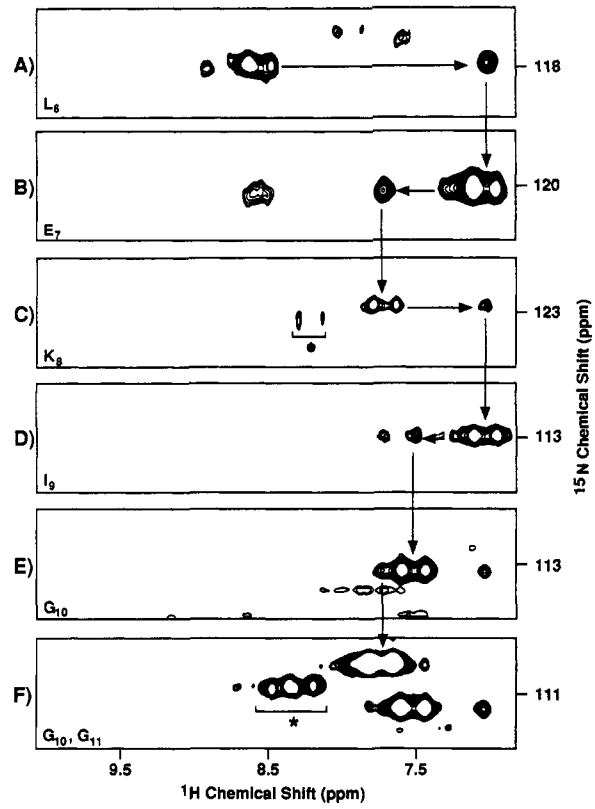

FIGURE 6: Contour plots of 2D ^{15}N-directed NOE spectra obtained from F_{ab}' complexes with peptides ^{15}N-labeled at residues L_6–G_{11}. Spectra were acquired with a 2D HMQC-NOE pulse sequence using a jump–return pulse for H_2O suppression at the end of the NOE mixing period; no ^{15}N decoupling during acquisition was employed. The mixing time was 50 ms for all spectra except that shown in panel B (30 ms). The amide/aromatic ^{1}H chemical shift region plotted in all spectra is 6.8–10.0 ppm; the ω_1 ^{15}N chemical shift region shown varies while the ω_1 scale of all plots is the same. Spectra were recorded at 308 K and ^{1}H and ^{15}N Larmor frequencies of 600 and 60.8 MHz, respectively. A total of 32–64 t_1 points and 4096–16 384 t_2 points were acquired per data set. Approximately 1600–2176 transients were collected per t_1 point using a 2-s recycle delay and a typical acquisition time of 0.4 s. The 2D data were processed using 20–35 Hz of exponential line broadening in ω_2 and a phase-shifted sine bell (75–90°) in ω_1. Asterisks indicate additional resonances due to unbound peptide observed from samples containing excess free peptide. In panel F, free resonances due to both labeled residues, G_{11} and G_{10} (the latter resonance is folded along ω_1), are observed. Typical F_{ab}' and peptide concentrations were 0.2–1.0 mM. The arrow scheme is described in the text.

pathway of sequential NOE connectivities in the peptide is indicated by the arrows in Figure 6 according to

NH(i) source peak → NH–NH(i,i+1) NOE peak →NH(i+1) source peak → etc.

Only a single NOE cross peak is observed for the complex of the peptide labeled with ^{15}N at K_8 (Figure 6C) because the E_7 and I_9 NH proton resonances are degenerate. However, the sequential NH–NH NOEs between E_7 and K_8, and I_9 and K_8, are evidenced in Figure 6B,D. The sequential NH–NH NOEs extended without interruption from residues F_5 through G_{11} in the bound peptide. The assignment of the NOE resonances to sequential NH–NH interactions in the peptide can be made with great confidence due to the reversible nature of the observed cross-relaxation pathways. In all cases, if an NOE was observed from the amide proton of residue i resonating at frequency ω_i to a proton resonating at frequency ω_j which coincided with the frequency of the amide proton of residue j (where $j = i \pm 1$), then an NOE was also observed from the latter proton to one with frequency ω_i.

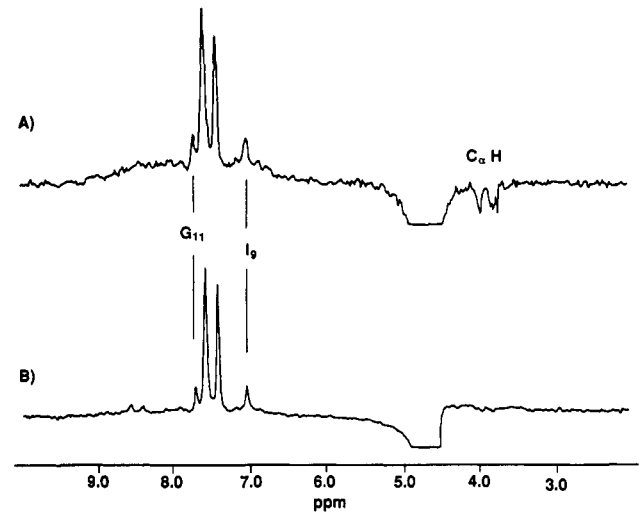

FIGURE 7: ^{15}N-edited NOE spectra obtained at 600 MHz and 308 K with a 50-ms mixing time. Spectrum A was recorded from a sample of ^{15}N-labeled G_{10} peptide–F_{ab}' complex. Spectrum B was recorded under conditions identical to those of spectrum A from a sample of F_{ab}' complexed with peptide similarly ^{15}N-labeled but also α-deuterated at G_{10} and G_{11} and perdeuterated at I_9. Both FIDs were apodized with 6 Hz of Lorentzian broadening before Fourier transformation.

The ^{13}C-edited NOE results confirm the intraresidue nature of certain NOEs involving G_{10}. C_αH–NH NOEs are observed in spectra obtained from complexes of F_{ab}' with either ^{15}N-labeled G_{10} or $^{13}C_\alpha$-labeled G_{10} peptides and indicate a relatively short distance between the C_α and amide protons, or short intraresidue $d_{N\alpha}$, for this residue. The relative intensities of the $d_{NN}(i,i+1)$ versus the intraresidue $d_{N\alpha}$ NOEs shown in Figure 4 indicates that the distances between both C_α protons and the amide proton of G_{10} are somewhat shorter than the sequential d_{NN} (G_{10}–I_9 and G_{10}–G_{11}) distances. The ^{13}C-edited NOE spectrum (Figure 5) indicates the occurrence of an intraresidue (G_{10}) $d_{N\alpha}$, as well as a sequential $d_{\alpha N}$ (G_{10}–G_{11}) NOE; the intensity of the sequential $d_{\alpha N}$ NOE connectivity is less than the intraresidue $d_{N\alpha}$ NOE. The relatively intense $d_{NN}(i,i+1)$ NOEs (G_{10}–I_9 as well as G_{10}–G_{11}) along with the strong intraresidue $d_{N\alpha}$ and weaker interresidue $d_{\alpha N}$ NOEs which have been observed and discussed above suggest that the backbone dihedral angles at G_{10} are in the α region of ϕ,ψ space. Due to the characteristic upfield C_αH chemical shifts of the glycines, minimal problems due to overlap with the H_2O resonance were encountered at 308 K. This facilitated the intra- versus interresidue NOE analysis presented here for residue G_{10} of the bound peptide.

NOE measurements involving glycine amide protons must always be interpreted with some caution due to potential problems with spin diffusion through the glycine α-protons (Redfield & Papastavros, 1990). The maximum value of $d_{N\alpha}(i,i)$ for a glycine residue is approximately 2.7 Å (Wüthrich, 1986), but typically the distance will be even shorter. In principle, therefore, the glycine α-protons can have a significant influence on the cross-relaxation behavior between the glycine amide proton and other nearby protons. Specific deuteration studies of the peptide–F_{ab}' complex have indicated that the sequential NH–NH(i,i+1) NOEs involving at least three residues of the bound peptide, I_9, G_{10}, and G_{11}, do *not* arise through indirect magnetization transfer through their respective α-protons (Tsang et al., 1990b). This is based upon the fact that substitution of deuterium at the G_{10} and G_{11} C_α positions and perdeuteration of residue I_9 enhanced rather than decreased the magnitude of the measured G_{10}–G_{11} and G_{10}–I_9 d_{NN} NOEs (Tsang et al., 1990b). This may be seen by com-

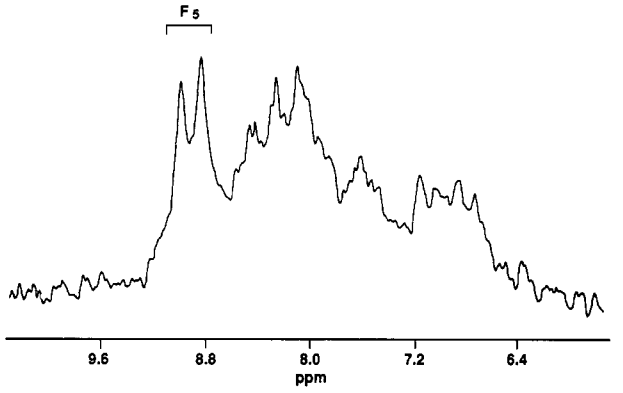

FIGURE 8: ^{15}N-edited NOE (35-ms mixing time) spectrum recorded at 308 K and 600 MHz from a complex of ^{15}N-labeled F_5 peptide with F_{ab}'. Approximately 27 000 transients were acquired using a recycle delay and acquisition time of 2 and 0.4 s, respectively. The spectrum was processed using 15 Hz of Lorentzian broadening. The underlying intensity is due to natural abundance ^{15}NH signals from F_{ab}'.

paring the two ^{15}N-edited NOE spectra shown in Figure 7. The spectrum of Figure 7A was recorded from F_{ab}' complexed with ^{15}N-labeled G_{10} peptide, while the spectrum of Figure 7B was obtained from a complex containing peptide ^{15}N-labeled at G_{10} and deuterated as described above at residues G_{10}, G_{11}, and I_9 as well. The NOEs around 4 ppm disappear in Figure 7B due to deuteration, confirming their assignment as the $C_\alpha H$ protons of G_{10}. Hence, the sequential d_{NN} NOEs among the I_9, G_{10}, and G_{11} residues are concluded to result from direct magnetization transfer.

The pattern of amide/aromatic NOEs observed for the D_4 and F_5 ^{15}N-labeled complexes was quite different from that described above for the L_6–G_{11} residues. The ^{15}N-edited NOE spectra recorded with 30–50-ms mixing times from complexes labeled at residues D_4 and F_5 did not show evidence of a sequential d_{NN} (D_4–F_5) NOE. This is demonstrated by the spectrum (Figure 8) of a complex of F_{ab}' with peptide ^{15}N-labeled at F_5. A large number of NOEs between the F_5 amide proton and nearby protons of the peptide or F_{ab}' are observed, but no significant resonance intensity is seen at the D_4 amide proton frequency in this or other NOE spectra recorded from the F_5-labeled complex. It is also difficult to determine whether a sequential NH–NH NOE exists between residues F_5 and L_6 from the spectrum of Figure 8, although this NOE appears to be present in Figure 6A where observation is via a ^{15}N label at the amide of L_6. The large number of NOEs to amide or aromatic protons in the spectrum of Figure 8 probably reflects a high overall density of protons surrounding F_5 in the antibody complex. Similar observations were made for complexes with peptide labeled at D_4 and to a lesser extent, L_6. Since all three of these side chains are critical for antibody binding (Fieser et al., 1987; Scott & Smith, 1990), the higher NOE density observed may indicate more intimate interactions with residues on the antibody than is the case for other amino acids of the peptide.

The conversion of NOE measurements into a set of internuclear distance constraints is a problematic step in NMR studies of systems in the long correlation time regime. In a transient NOE experiment the magnetization transfer behavior has a multiexponential dependence on the length of the mixing time, and it is only in the short mixing time limit that the measured NOE intensities are directly proportional to the cross-relaxation rates (Macura & Ernst, 1980). Internuclear distances are usually derived from the cross-relaxation rates by comparison of the intensity of the NOE between spins with unknown separation to that of the NOE between a pair of reference spins separated by a fixed distance; this method assumes that the motional correlation times are similar for the two pairs of spins. This procedure, which is standard practice in studies of small proteins and nucleic acid fragments, is not feasible in studies of larger systems such as the F_{ab}'–peptide complex. Relatively poor sensitivity in the latter case is a major practical concern, and it is usually necessary to employ mixing times in the NOE experiment which are well outside the short mixing time regime in order to observe NOEs with a reasonable signal-to-noise ratio. In such cases, it is not possible to employ the initial rate approximation to determine the cross-relaxation rates. Another problem is that it is difficult to convert NOE measurements between backbone amide protons to internuclear distances because there is no suitable calibration for this measurement unless the local secondary structure can be established independently.

In light of these problems, it is necessary to employ a different strategy in order to interpret the measured NOEs in the F_{ab}'-bound peptide. This strategy is based on determining the ratio of integrated resonance intensities of an NOE peak to its source peak (i.e., the resonance for the nucleus from which the magnetization was transferred), with both intensities measured at the same mixing time. This ratio is then compared to theoretical simulations for known geometrical arrangements of nuclei. The rationale for this strategy is discussed below. It is necessary to take the ratio of intensities since the absolute intensities are meaningless. A ratio of intensities of the NOE peak at a given mixing time to the relevant source peak at zero mixing time would be an equally useful parameter, but experimental difficulties in recording the zero mixing time spectra make this approach less practical. The advantages of using the intensity ratios for eliminating the effects of external relaxation processes and for facilitating the measurement of cross-relaxation rates using an initial rate approximation have been described previously (Bodenhausen & Ernst, 1982; Macura et al., 1986). An advantage of the isotope-edited NOE experiment is that integration of both the NOE and source peaks is usually straightforward; in unedited spectra, the likelihood of overlap of resonances with similar chemical shifts makes the integration of source peak intensity impossible in most cases.

Theoretical NOE calculations were carried out using proton coordinates derived from the protein crystal structures of poplar plastocyanin (Guss & Freeman, 1983) and *T. zostericola* myohemerythrin (Sheriff et al., 1987), which are representative β-sheet and α-helical proteins, respectively. The cross-relaxation behavior as a function of mixing time in a transient NOE experiment was calculated for all pairs of sequentially adjacent backbone amide protons for each set of proton coordinates; the calculations were done using the full relaxation matrix to account for all spin diffusion effects. No internal motions were included in the calculations, except for methyl group rotation; isotropic tumbling with a correlation time τ_c for the entire molecule was assumed. Ratios of NOE peak to source peak intensities were determined for selected values of τ_c (chosen to be in the range expected for an F_{ab}–peptide complex) and the mixing time τ_m. For each combination of τ_c and τ_m, the intensity ratio data were plotted versus the internuclear distance for the corresponding pairs of amide protons.

Some results of the theoretical NOE intensity ratio calculations are presented in Figure 9; data are shown for two correlation times, 15 and 20 ns, and two mixing times, 35 and 50 ms. The various data were calculated for a Larmor fre-

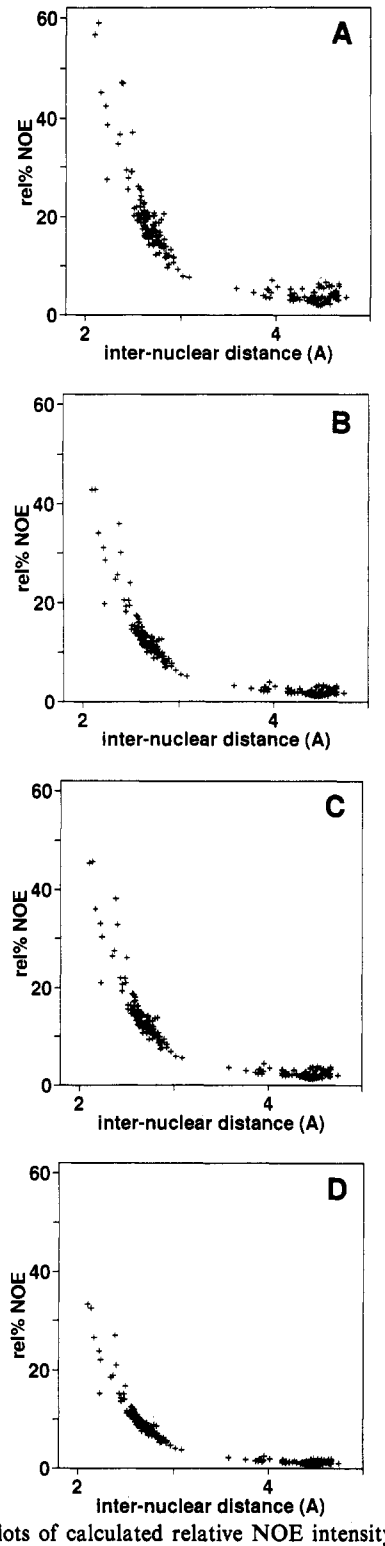

FIGURE 9: Plots of calculated relative NOE intensity (sequential NH–NH NOEs) versus interproton distances at 600 MHz. The proton coordinates were derived from the protein data bank files for *T. zostericola* myohemerythrin and poplar plastocyanin proteins as described in the text. (Curve A) τ_m = 50 ms and τ_c = 20 ns. (Curve B) τ_m = 35 ms and τ_c = 20 ns. (Curve C) τ_m = 50 ms and τ_c = 15 ns. (Curve D) τ_m = 35 ms and τ_c = 15 ns. The curves were calculated for a ^{1}H frequency of 600 MHz. Theoretical intensities were calculated as a ratio of the integrated NOE intensity to the source peak intensity at the same mixing time.

quency of 600 MHz, and the following values: τ_c = 20 ns, τ_m = 50 ms (Figure 9A); τ_c = 20 ns, τ_m = 35 ms (Figure 9B); τ_c = 15 ns, τ_m = 50 ms (Figure 9C); τ_c = 15 ns, τ_m = 35 ms (Figure 9D). The rotational correlation time for the F_{ab}'–peptide complex is expected to be approximately 20 ns, as derived from nanosecond fluorescence polarization spectroscopy (Oi et al., 1984; Yguerabide et al., 1970) and corrected for the temperature employed in the present study. This value also agrees with an experimental correlation time of 20 ns determined by ESR for an F_{ab}–hapten complex (Anglister et al., 1984). In view of the experimental ^{1}H and ^{15}N line width data which indicate that there is a mobility gradient along the peptide backbone, simulations are shown for two values of the correlation time, τ_c, to demonstrate the expected trend in the NOEs in the case in which regions of the peptide have some internal mobility. The simulations clearly demonstrate that, for NOE intensity ratios above a certain threshold value, there is a distinct correlation between the intensity ratio and the internuclear separation of adjacent backbone amide protons. Within the limitations of the theoretical calculations, this intensity/distance correlation can be used to put a conservative upper limit on the internuclear separation of the adjacent amide protons for which experimental NOE data are available.

The relative integrated intensities of the NOE resonances observed in the 1D ^{15}N-edited NOE spectrum of Figure 4 appear to be ~45% and 29% for the intraresidue G_{10} amide to α-proton NOEs (3.98 and 3.83 ppm, respectively). The interresidue NOEs between this and the amide protons of G_{11} (7.72 ppm) and I_9 (7.05 ppm) are each about 11%. The relative intensities of the G_{10} amide proton NOEs then appear to be $d_{N\alpha} > d_{NN}$ (G_{10}–I_9) ~ d_{NN} (G_{11}–G_{10}). The relative intensities were estimated for the remaining residues [for which obvious, identifiable d_{NN}(i,i+1) NOEs were measured] by integrating the resonances seen in the appropriate rows of the 2D ^{15}N-edited NOE data sets as well as the corresponding 1D spectra recorded from these complexes. All integrated intensities were corrected for the jump–return excitation profile used in the NOE measurements. The experimental NOE intensity ratios were estimated to be 10–15%, with an estimated error of several percent, for the NH–NH sequential NOEs between all residues from L_6 to G_{11}. As discussed previously, sequential NH–NH NOEs could not be observed in spectra of the F_{ab}' complex with peptides labeled at residues D_4 and F_5. Based upon the simulated relative NOE intensity curves (Figure 9) and the magnitude of the experimental NOE intensity ratios for the complex, a conservative upper limit of the $d_{NN}(i,i+1)$ distance in the bound peptide is 3 Å for residues F_5–G_{11}.

The present studies of an F_{ab}'–peptide complex show that direct NOEs between protons separated by less than ca. 3 Å can be readily observed for proteins and protein complexes of molecular mass up to ~50 kDa using isotope-edited NMR techniques. By measurement of the relative intensities of the NOE peaks and source peaks, reasonable estimates of upper distance bounds between backbone protons can be obtained with the aid of relaxation matrix simulations. The measurement of longer range NOEs, between protons separated by more than 3 Å, is more difficult due to the relatively broad resonances of the F_{ab}'–peptide complex and the corresponding sensitivity problems that result. This situation may be improved through the use of a specific peptide deuteration strategy (Tsang et al., 1990b) to enhance the magnitude and buildup properties of the NOEs. Selective deuteration could facilitate the measurement of medium- and long-range NOEs that would be invaluable for structure determination.

Even in the absence of long-range or medium-range NOEs, the observed interresidue NOEs provide important information about the conformation of the peptide when bound to the antibody. It is reasonable to assume that the conformational space accessible to the peptide is highly restricted within the

antibody combining site, i.e., that it adopts a single conformation or a small family of very similar conformations in the binding site. Indeed, X-ray crystallographic studies of a peptide bound to the F_{ab} fragment of the antipeptide antibody B13I2 show that the peptide epitope forms a single well-defined β-turn in the antibody pocket (Stanfield et al., 1990). It is also likely that most, if not all, of the residues within the peptide epitope will adopt backbone dihedral angles in low-energy regions of ϕ,ψ space. Of the allowed regions of the Ramachandran plot, only the α_R and α_L regions have $d_{NN}(i,i+1)$ distances less than 3 Å (Billeter et al., 1982; Wright et al., 1988). Thus, the observation of short sequential backbone NH(i)–NH(i+1) distances (<3 Å) for all residues between F_5 and G_{11} in the complex of the peptide MHKDFLEKIGGL with the antipeptide F_{ab}' B13A2 strongly implies that the backbone in this region of the peptide adopts an approximately helical structure when bound to the antibody. An acknowledged shortcoming of our present experiments is our inability to observe characteristic medium-range intrapeptide NOEs that could unambiguously confirm the stabilization of a helical conformation in the antibody combining site. However, the observation of short sequential $d_{NN}(i,i+1)$ distances over most of the epitope strongly suggests that such a structure is formed. Our present data provide no information about side-chain conformations of the bound peptide or about the backbone conformations between M_1 and F_5.

Using isotope-edited NMR experiments, we have obtained strong evidence that the peptide MHKDFLEKIGGL derived from the C-helix of myohemerythrin adopts helical backbone conformations between residues F_5 and G_{11} in the combining site of the F_{ab}' fragment of B13A2. This antibody was raised against a 19 amino acid peptide immunogen corresponding to the entire C-helix. The fact that residues F_5–G_{11} of the peptide are helical in the X-ray structure of myohemerythrin may help to explain the reported cross-reactivity of B13A2 with the native protein (Fieser et al., 1987). Earlier NMR studies of the 19-residue peptide immunogen in aqueous solution (Dyson et al., 1988) revealed a propensity for nascent helical conformations in the region of the epitope recognized by the antibody B13A2. Thus it appears that the conformational ensemble that includes the nascent helix, characterized by weak $d_{NN}(i,i+1)$ and $d_{\alpha N}(i,i+2)$ NOE connectivities, is driven toward a helical state upon binding to the antibody. Again, we stress that we have no information at this stage about the backbone conformation between F_5 and D_4, which also forms part of both the NMR and immunologically defined epitope.

Conclusions

The ability to physically characterize the structure and dynamics of the bound antigen in an antibody–antigen complex is relevant to an understanding of antigen–antibody interactions in general. One specific question regarding the interactions of antipeptide antibodies concerns the relative conformations of the peptide and protein antigens when they are bound to an antibody cross-reactive with both. In these studies, we have focused upon the interactions and conformational properties of the bound peptide antigen using isotope-edited NMR techniques. These techniques have allowed the specific observation of the peptide component of these complexes and yielded information regarding both the dynamic and structural properties of the antibody-bound antigen. Differences in relative backbone mobility are observed which are consistent with immobilization of residues within the epitope upon binding to the antibody. In addition, isotope-edited NOE experiments indicate that residues F_5–G_{11} adopt a folded conformation in the antibody binding site such that short sequential amide–amide proton distances exist. Despite technical difficulties usually associated with application of solution NMR techniques to study high molecular weight systems such as this F_{ab}'–peptide complex, it appears that information on conformation can be obtained by observation of short-range NOE interactions. While a full structural characterization of the bound peptide would require additional medium- to long-range NOE constraints, it appears that the epitope of the peptide MHKDFLEKIGGL most likely adopts a helical conformation on binding to the antibody B13A2. The ability to obtain and interpret NOE information from protons separated by longer distances than ~3 Å will require development and application of further methodology such as deuteration of the antibody and/or selective deuteration of the peptide. Isotope-edited NMR methods of the type used successfully here to study antibody–peptide complexes should find widespread applications in studies of ligand–receptor interactions.

Acknowledgments

We thank L. L. Tennant and R. T. Samodal for their aid in preparing the peptide and antibody samples used in these experiments. We thank Drs. U. C. Singh and K. Ramnarayan for their assistance with generation of the proton coordinates from protein databank files. We also thank Drs. H. J. Dyson, A. G. Palmer, and P. Yip for helpful discussions.

References

Anglister, J. (1990a) *Q. Rev. Biophys. 23*, 175–203.
Anglister, J., & Zilber, B. (1990b) *Biochemistry 29*, 921–928.
Anglister, J., Frey, T., & McConnell, H. M. (1984) *Biochemistry 23*, 1138–1142.
Anglister, J., Bond, M. W., Frey, T., Leahy, D., Levitt, M., McConnell, H. M., Rule, G. S., Tomasello, J., & Whittaker, M. (1987) *Biochemistry 26*, 6058–6064.
Anglister, J., Jacob, C., Assulin, O., Ast, G., Pinker, R., & Arnon, R. (1988) *Biochemistry 27*, 717–724.
Anglister, J. A., Levy, R., & Scherf, T. (1989) *Biochemistry 28*, 3360–3365.
Arnon, R. (1986) *Trends Biochem. Sci. 11*, 521–524.
Aue, W. P., Bartholdi, E., & Ernst, R. R. (1976) *J. Chem. Phys. 64*, 2229–2246.
Bax, A., & Subramanian, S. (1986) *J. Magn. Reson. 67*, 565–569.
Bax, A., Griffey, R. H., & Hawkins, B. L. (1983) *J. Magn. Reson. 55*, 301–315.
Benoiton, L. (1962) *Can. J. Chem. 40*, 570–572.
Billeter, M., Braun, W., & Wüthrich, K. (1982) *J. Mol. Biol. 155*, 321–346.
Bodenhausen, G., & Ruben, D. J. (1980) *Chem. Phys. Lett. 69*, 185–189.
Bodenhausen, G., & Ernst, R. R. (1982) *J. Am. Chem. Soc. 104*, 1304–1309.
Dyson, H. J., Rance, M., Houghten, R. A., Wright, P. E., & Lerner, R. A. (1988) *J. Mol. Biol. 201*, 201–217.
Erickson, B. W., & Merrifield, R. B. (1973) *J. Am. Chem. Soc. 95*, 3757–3763.
Fesik, S. W., Luly, J. R., Erickson, J. W., & Abad-Zapatero, C. (1988) *Biochemistry 27*, 8297–8301.
Fieser, T. M., Tainer, J. A., Geysen, H. M., Houghten, R. A., & Lerner, R. A. (1987) *Proc. Natl. Acad. Sci. U.S.A. 84*, 8568–8572.
Glasel, J. A., & Borer, P. N. (1986) *Biochem. Biophys. Res. Commun. 141*, 1267–1273.

Glaudemans, C. P. J., Lerner, L., Daves, G. D., Jr., Kovâc, P., Venable, R., & Bax, A. (1990) *Biochemistry 29*, 10906–10911.
Goldman, M. (1984) *J. Magn. Reson. 60*, 437–452.
Griffey, R. H., & Redfield, A. G. (1987) *Q. Rev. Biophys. 19*, 51–82.
Guss, J. M., & Freeman, H. C. (1983) *J. Mol. Biol. 169*, 521–563.
Houghten, R. A. (1985) *Proc. Natl. Acad. Sci. U.S.A. 82*, 5131–5135.
Ito, W., Nishimura, M., Sakato, N., Fujio, H., & Arata, Y. (1987) *J. Biochem. (Tokyo) 102*, 643–649.
Itoh, M., Hagiwara, D., & Kamiya, T. (1975) *Tetrahedron Lett. 49*, 4393–4394.
Jeener, J., Meier, B. H., Bachmann, P., & Ernst, R. R. (1979) *J. Chem. Phys. 71*, 4546–4553.
Keepers, J. W., & James, T. L. (1984) *J. Magn. Reson. 57*, 404–426.
Lerner, R. A. (1982) *Nature 299*, 592–596.
Lerner, R. A. (1984) *Adv. Immunol. 36*, 1–44.
Levy, R., Assulin, O., Scherf, T., Levitt, M., & Anglister, J. (1989) *Biochemistry 28*, 7168–7175.
Live, D. H., Davis, D. G., Agosta, W. C., & Cowburn, D. (1984) *J. Am. Chem. Soc. 106*, 1939–1941.
Macura, S., & Ernst, R. R. (1980) *Mol. Phys. 41*, 95–117.
Macura, S., Farmer, B. T., II, & Brown, L. R. (1986) *J. Magn. Reson. 70*, 493–499.
Marion, D., Ikura, M., & Bax, A. (1989) *J. Magn. Reson. 84*, 425–430.
Messerle, B. A., Wider, G., Otting, G., Weber, C., & Wüthrich, K. (1989) *J. Magn. Reson. 85*, 608–613.
Oi, V. T., Vuong, T. M., Hardy, R., Reidler, J., Dangl, J., Herzenberg, L. A., & Stryer, L. (1984) *Nature 307*, 136–140.
Olejniczak, E. T. (1989) *J. Magn. Reson. 81*, 392–394.
Olejniczak, E. T., Gampe, R. T., & Fesik, S. W. (1986) *J. Magn. Reson. 81*, 28–41.
Otting, G., & Wüthrich, K. (1990) *Q. Rev. Biophys. 23*, 39–96.
Palmer, A. G., III, Cavanagh, J., Wright, P. E., & Rance, M. (1991) *J. Magn. Reson. 93*, 151–170.
Palmer, A. G., III, Skelton, N. J., Chazin, W. J., Wright, P. E., & Rance, M. (1992) *Mol. Phys. 75*, 699–711.
Plateau, P., & Guéron, M. (1982) *J. Am. Chem. Soc. 104*, 7310–7311.
Rance, M., Wright, P. E., Messerle, B. A., Field, L. D. (1987) *J. Am. Chem. Soc. 109*, 1591–1593.
Redfield, A. G., & Papastavros, M. Z. (1990) *Biochemistry 29*, 3509–3514.
Scott, J. K., & Smith, G. P. (1990) *Science 249*, 386–390.
Shaka, A. J., Keeler, J., Frenkiel, T., & Freeman, R. (1983) *J. Magn. Reson. 52*, 335–338.
Sheriff, S., Hendrickson, W. A., & Smith, J. L. (1987) *J. Mol. Biol. 197*, 273–296.
Singh, U. C., Weiner, P. K., Caldwell, J. W., & Kollman, P. A. (1986) University of California, San Francisco, CA.
Stanfield, R. L., Fieser, T. M., Lerner, R. A., & Wilson, I. A. (1990) *Science 248*, 712–719.
Steward, M. W., & Howard, C. R. (1987) *Immunol. Today 8*, 51–58.
Tropp, J. (1980) *J. Chem. Phys. 72*, 6035–6043.
Tsang, P., Fieser, T. M., Ostresh, J. M., Lerner, R. A., & Wright, P. E. (1988) *Pept. Res. 1*, 87–92.
Tsang, P., Fieser, T. M., Ostresh, J. M., Houghten, R. A., Lerner, R. A., & Wright, P. E. (1990a) in *Frontiers of NMR in Molecular Biology*, pp 63–73, A. R. Liss, Inc., New York.
Tsang, P., Wright, P. E., & Rance, M. (1990b) *J. Am. Chem. Soc. 112*, 8183–8185.
Tsang, P., Wright, P. E., & Rance, M. (1990c) *J. Magn. Reson. 88*, 210–215.
Tsang, P., Rance, M., & Wright, P. E. (1991) *Methods Enzymol. 203*, 241–261.
Van Regenmortel, M. H. W. (1987) *Trends Biochem. Sci. 12*, 237–240.
Wagner, G. (1989) *Methods Enzymol. 176*, 93–113.
Walter, G. (1986) *J. Immunol. Methods 88*, 149–161.
Wilson, I. A., Stanfield, R. L., Rini, J. M., Arevalo, J. H., Schulze-Gahmen, U., Fremont, D. H., & Stura, E. A. (1991) in *Catalytic Antibodies*, pp 13–39, Ciba Foundation Symposium 159, Wiley, Chichester.
Wright, P. E., Dyson, H. J., & Lerner, R. A. (1988) *Biochemistry 27*, 7167–7175.
Wüthrich, K. (1986) *NMR of Proteins and Nucleic Acids*, Wiley, New York.
Yguerabide, J., Epstein, H. F., & Stryer, L. (1970) *J. Mol. Biol. 51*, 573–590.
Zilber, B., Scherf, T., Levitt, M., & Anglister, J. (1990) *Biochemistry 29*, 10032–10041.